Mehran University Research Journal of Engineering and Technology

https://doi.org/10.22581/muet1982.3026

2024, 43(3) 78-88

Martensitic transformation temperature modification of Fe-SMA for efficient medical implants

Muhammad Muneeb Rasheed *, Ahmed Saif, Rana Atta ur Rahman, Muhammad Ali Nasir, Shahid Mehmood, Muhammad Usman, Abdul Moiz Rao

Department of Mechanical Engineering, University of Engineering and Technology, Taxila, Pakistan

* Corresponding Author: Muhammad Muneeb Rasheed, Email: mohammadmuneebrasheed@gmail.com

Received: 15 September 2023, Accepted: 25 Jun 2024, Published: 01 July 2024

K E Y W O R D S

Fe-SMA

DSC (Differential Scanning Calorimetry)

Phase Transformation

Brine Quenching

Heat Treatment

Austenite Start Temperature (A_s)

A B S T R A C T

Nickel-Titanium alloys or Nitinol shape memory alloys have applications in various fields like biomedical, agriculture, pharmaceutical, civil, and mechanical engineering. Ferrous-based shape memory alloys (Fe-SMAs) do not possess excellent properties like that of Nitinol. In recent times, Fe-SMAs have been under consideration in the research field to enhance their shape memory properties because of their cost-effectiveness, corrosion resistance, biocompatibility, and high mechanical strength. Fe-SMAs are limited in their applications in the human body due to high austenite start temperature (A_s) even though they are biocompatible and being considered for temporary biodegradable implant applications. Several factors affect the phase transformation temperature of Fe-SMA, like alloy composition and heat treatment conditions. Some of the techniques that are useful to reduce the A_s are quenching, solid solution treatment, ternary element addition, alloying, and thermal-mechanical treatment. In this study, the quenching with brine solution is used to reduce A_s of Fe-15Mn-10 Cr-8Ni-4Si (wt. %). The phase transformation is observed using Differential Scanning Calorimetry (DSC). The best result from experimentation of all the samples collected as A_s reduced from 93ºC to 39.02ºC which is very close to the temperature of the human body. The results of this study exhibit significant potential for advancement in the application of Fe-SMAs in the biomedical field for permanent implants in cardiovascular and orthopaedic applications.

1. Introduction

Shape memory alloys are the alloys that keep the memory of their shape. This effect makes shape memory alloys superior to other materials. After applying stress on a shape memory alloy, it undergoes deformation, and when the stress is removed, the shape recovery effect can be observed when it reaches its austenite start temperature (A_s). Their shape-recovering response is of the order of milliseconds through the achievement of phase transformation temperature [1].

Shape memory alloys (SMAs) have recently got much attention as smart materials. Several approaches have been explored to leverage the unique performance of SMA, such as shape memory effect (SME), superelasticity (SE), high damping, and mechanical properties. Today, Nitinol (NiTi) and Fe-SMAs have been widely used in various fields because of their reliability and convenience. NiTi shape memory alloys are important materials for many industrial as well as biomedical applications, primarily due to their shape memory effect associated with the transition from austenitic to the martensitic phase structure and from martensitic to austenitic structure. Nitinol SMAs can be easily transported and stored at room temperature.

In this study, Fe-based SMA is selected due to its advantages such as good biocompatibility, cost-effectiveness, and good mechanical performance. As

evident from the literature, NiTi SMAs are being used in biomedical applications but are very costly. Fe-SMAs exhibit good biocompatibility and shape recovery properties comparable with NiTi SMAs. High A_s is also a limiting factor regarding Fe-SMA human implant applications. Quenching with brine solution is used to lower the (A_s) of the smart material to the extent that it approaches the optimal human body temperature. With this, it can be used in a wide range of biomedical applications and is an excellent alternative for NiTi SMAs as they exhibit excellent corrosion resistance properties and biocompatibility.

Pseudo elasticity (PE) or superelasticity (SE) and Shape memory effect (SME) are the exceptional properties that make shape memory alloys superior to other materials. Superelasticity is a property of this material that allows it to remember its shape after stress loading. The stress-strain curve response of shape memory alloys shows super elasticity [2]. In superelastic materials, the alloy is in the austenite phase in no loading condition and when load is applied, the martensite is detwinned. When the alloy is unloaded, the detwinned martensite is converted to austenite without requiring any thermal change. The shape memory effect (SME) is the behaviour when deformation happens in a material, and it recovers its initial shape when heat is applied above a specific characteristic transformation temperature. The fundamental difference between the superelasticity and shape memory effect is the residual stress after the stress unloading. In superelasticity, there is no residual stress as the austenite state is achieved entirely just after the unloading [3]. However, there is residual stress present in the material in the shape memory effect, due to which the complete austenite phase is not achieved. Both Pseudo elasticity and SME can be observed in the following Fig. 1 [3]. However, there is residual stress present in the material in the shape memory effect, due to which the complete austenite phase is not achieved. Both Pseudo elasticity and SME can be observed in the following Fig. 1.

The residual stress is to be removed for the reverse transformation and the temperature must be higher than the A_s for complete transformation. Austenite finish temperature is the final requirement of the austenite phase in the shape memory effect. In the forward transformation, the austenite is converted into twinned martensite due to the temperature decrease as martensite start, M_s and martensite finish M_f temperatures are achieved [4]. Then, due to the stress loading, twinned martensite converts into detwinned martensite. Then the recovery process or the reverse transformation occurs in which detwinned martensite converts into austenite after achieving the $A_s$and A_f.

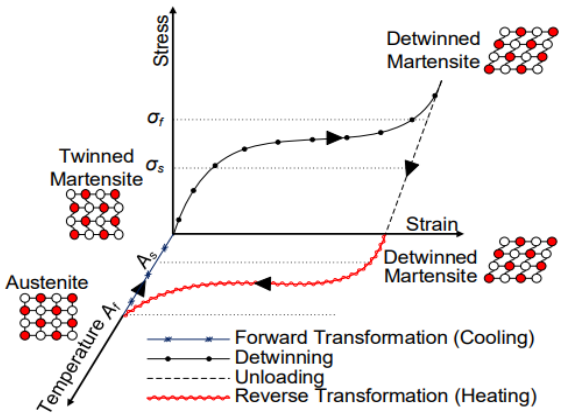

Fig. 1. The Shape Memory Effect Process of A Typical SMA [4].

Bujoreanu found several parameters affecting the microstructure and the phase transformation behaviour of the Fe-SMA, like alloy composition, quenching temperature, quenching time and quenching method [5]. He also found the point where the change in the elastic modulus occurred during heating tend to increase marginally with an increase in the temperature of quenching and to decrease with an increase in enduring elongation with the help of dilatometry. Phase transformation temperatures and microstructure of an alloy depend on heat treatment conditions and the composition of the alloy [6]. Saud also found that oil up-quenched is the best quenching medium as it gives the lowest A_s for a Cu-Al-Ni-Fe-SMA. The highest difference in the phase transformation energy is found when it is cooled with brine solution. Bikas C. found in a study with a highly pure composition of Fe, Mn, Si, Cr, Ni and Cu (99.95%) that different quenching conditions of Fe-SMAs will affect the phase transformation temperatures and the austenite phase transformation, which controls the pseduoelastic behaviour of the SMA [7]. The study reported crack formation due to rapid cooling during quenching and no effect of grain boundary precipitation is reported on the superelasticity behaviour.

Bikas Maji reported that with pure composition of Fe, Mn, Si, Cr, Ni and Cu (99.95%), different quenching conditions of Fe-SMAs will affect the phase transformation temperatures of the austenite phase transformation, which controls the superelasticity or Pseudo elasticity behaviour of the SMA. He also found that copper addition decreases the A_s, and with the austenite phase stability, the weakening of the shape recovery effect is observed. Also, ageing at 750ºC for two hours decreased the A_s from 85.8ºC to 73.6ºC [8]. Sakuma found that maximum uniform elongation can be achieved in inter-critically Heat-Treated Bainite-Transformed Steel with more time in the bainite phase. Carbon

content determines the austenite stability, and the addition of Si and Mn is found to enhance austenite stability without improving ductility and strength [9]. Caenegem found that less austenitic transformation is achieved with high C and low martensite start temperature (M_s). Carbon addition to Fe-SMAs increases the tensile strength, lowers the martensitic phase, and strain hardening [10]. Van Humbeeck found that optimum SME can be achieved through suitable alloy composition, stress-induced martensitic transformation should be without slip, $M_s >$ Neel Temperature, and stress-induced α'-martensite transformation should be prevented to avoid deterioration of SME [11].

SME of Fe-SMAs can be enhanced as C. Y. Zhang found that single-crystal Fe-SMA does not show Pseudo elasticity. Still, polycrystalline ones do, but martensitic transformation must be stress-induced and improved volume resistivity causes the improvement in martensitic transformation [12]. It is found in Fe-Mn-Si-Ni-Co SMA, and Pseudo elasticity only has partial applications as it is not that advantageous [13]. Rong found critical stress decrement to be enhancing SME, and for it, the optimum temperature is 973K and strain in the range of 2% to 3.5% is found to be optimal [14]. Akhundzada found annealing at 923.15K to be optimum for maximum SME and lower SME is reported at higher annealing temperatures [15]. M_s and A_s for SMAs can be predicted through artificial neural networks, as demonstrated by Omer Eyercioglua [16]. M_s and A_s conditions for polycrystalline Fe-9% Cr-5%Ni-14%Mn-6%Si were also predicted by Tanaka through J_3-theory [17].

For Fe-Mn-Si-Cr-Ni-VC, uniaxial deformation affects phase transformation behaviour, as found by Weber [18] and also reported by Cao and Iwamoto for Fe-28Mn-6Si-5Cr alloy [19], [20]. These alloys are costly but advantageous for lost prestress recovery and are mainly used in civil structures [21]. Ferromagnetic SMAs can be used as an alternative to Ni–Mn–Ga SMAs as they are more ductile and can be used in magnetic actuators and high-temperature applications [22]. Shape recoverability is reduced by increasing hold stress and decreasing back stress and it is assumed that there is a linear relation between martensitic volume fraction and back stress [23].

In a study using NiTi, Yeung found that the lowest A_s is obtained when the first ageing process is done on the specimen for 45 minutes [24]. The study is conducted with three different cooling conditions: air-cooled, water-quenched, and furnace-cooled. The highest value of hysteresis of reverse transformation is obtained when ageing is done at 450oC, and it is water quenched. The yielding theory describes how the shape memory alloy will behave inelastically in the martensite phase when the magnetic load is applied to it [25]. Residual stresses do not affect the phase transformation mechanism but affect transformation temperatures in the case of NiTi spring. Specimen location and difference of A_s and A_f affects austenite formation as Santhanam found [26]. The difference between the ultrafine-grained and coarser-grained microstructure of NiTi wire does not affect the Pseudo elastic cycling [27]. Thermomechanical training affects the shape recovery significantly when NiTi specimens are as-annealed. Partial transformation-induced internal stress is not effective in two way memory effect (TWME) and stress-assisted two-way memory effect (SATWME), but that of full transformation is favourable [28]. The deformation rate is not dependent on the temperature range in rich NiTi with 50.7% Ni as found by Grabe [29].

Lexcellent found the crystallographic theory of martensite to be effective for predicting the microstructure of Nitinol-based SMA [30]. Increasing the annealing temperatures after high-ratio differential speed rolling in the case of Fe-13.51. Mn-4.82 Si-8.32 Cr-3.49 Ni-0.15C results in a decrease in grain boundary density and recovery stress, resulting in an increase in recovery strain and grain size for the same conditions [31]. Increasing wall thickness in NiTi Nb pipe joints decreases A_s and has no significant effect on A_f, as found by L. Wang [32]. The ductility of Co-Ni–Ga alloys can be improved with suitable heat treatment along with increasing the martensitic transformation temperature [33]. Jiang found that Co63.5V17.0Si19.5 shows good strength and brilliant high-temperature martensitic transformation, and martensite stability needs improvement [34]. Fe-28Mn-6Si-5Cr SMA pipe joint is reported to exhibit change in failure mechanism at higher deformation rates [35] but using proper expansion methods at various deformation rates, higher strength is reported at high deformation rate with unidirectional pressing method [36]. The improvement in the strength can be predicted by pre-process strain monitoring [37].

Fe and Fe-based alloys are considered for their applications as temporary biodegradable implants in surgeries [38], cardiovascular applications, tracheal stents, and aneurysm treatment. These Fe-based metallic implants have some advantages like good strength, biocompatibility and high corrosion resistance. Fe-based alloy implants are favourable to biological compatibility, and they degrade slowly while retaining their mechanical properties to a duration that they do not recoil early. Compared to permanent implants, these iron-based implants or stents have fewer side effects like chronic swelling, and the arteries shrinking again. The degradation

property determines the performance of these Fe alloys. The ideal implant biodegradable for cardiovascular applications has strain hardening, ductility, and high strength [39]. Fe-SMAs can be used in cardiovascular and regenerative medicine in the surgical field if their biodegradable nature and performance can be achieved at a reliable level. Fe-SMAs do not have the same properties as Nitinol. Still, their features are similar to Nitinol to such an extent that they can be used as a replacement for Nitinol. Fe-SMAs have many applications in civil structures and mechanical components [40]. Their significance can be justified as they can provide a cheaper, corrosion-resistant [41], bio-compatible, and SME comparable to nitinol [42]. Fe-SMAs are superior to Nitinol if their hysteresis is considered as they have a wider hysteresis than Nitinol. Currently, Nitinol is being used in many biomedical engineering applications, and Fe-SMAs are not applicable in the human body due to high transformation temperatures [43]. The temperatures of solid solution treatment and ageing also affect the transformation temperatures [44]. It is evident in a study about Nitinol human body implant when Nitinol specimen with 550°C ageing after 800°C solid solution treatment and furnace cooling gives the least value of $A_s = -20$°C [24]. Table 1 shows the summary of the literature reporting the factors affecting the prediction and modification of the phase transformation behaviour of Fe-SMAs. different methods are reported for the modification of the phase transformation temperatures, like alloying addition, quenching, annealing, solution treatment, pre-stressing, residual stresses, and pipe joint expansion. Out of these reported methods, varying the quenching conditions is reported to result the promising outcome and, in this study, quenching conditions variation is selected to analyse the effect on the phase transformation temperatures of Fe-SMA.

Table 1

Literature review summary

#	Authors	Method	Findings	Ref.
1	Bujoreanu, Leandru G. et al.	Different Quenching Temperatures	Alloy composition and quenching conditions affect the microstructure and the phase transformation behaviour of the Fe-SMA.	[5]
2	Safaa N. Saud et al.	Quenching with Different Media	Oil up-quenched bath shows the least A_s as compared to the other quenching media used in the study.	[45]
3	Bikas Maji Madangopal Krishnan	Alloying Addition	Increasing the amount of copper and ageing is found to be decreasing A_s. Different quenching conditions also affected phase transformation and their temperatures.	[8]
4	Gu Q et al	Pre-Stressing	Stress-induced martensitic transformation can weaken SME, and optimum SME can be achieved using suitable alloy composition, $M_s >$Neel Temperate and no-slip formation.	[11]
5	Wang, Xiao Xiang Zhang, Chu Yang	Annealing and Solution Treatment	Single-crystal Fe-SMAs do not show Pseudo elasticity, but polycrystalline ones do with the condition of stress-induced martensitic transformation. Lowering the critical stress and Ausforming can enhance SME.	[13]
6	A. Akhondzadeh et al	Annealing Temperature Variation	Raising the annealing temperature while unloading causes less SME and annealing at 923.15K results in maximum SME.	[15]
7	O. Eyercioglu et al	Artificial Neural Networks	M_s and A_s for SMAs can be predicted through artificial neural networks.	[16]
8	Nishimura Fumihito et al	Transformation Temperatures Prediction	M_s and A_s conditions can be predicted for polycrystalline Fe-SMA through J_3-theory.	[17]
9	R. Santhanam et al	Residual Stresses	Residual stresses do not affect the phase transformation but their temperatures in the case of NiTi spring. Specimen location and $A_s - A_f$ affects austenite formation.	[26]
10	Wang L. et al	Pipe Joint Expansion	Increasing wall thickness in NiTi Nb pipe joints is decreasing A_s and having no significant effect on A_f.	[32]
11	K. W. K. K. Yeung et al	Thermal Treatment Optimization	The temperatures of solid solution treatment before ageing also affect the transformation temperatures.	[24]

2. Methodology

The shape memory alloy used in this study is a ferrous-based shape memory alloy with the composition of Fe-15Mn-10Cr-8Ni-4Si (wt. %). This alloy exhibits excellent damping properties along with good biocompatibility due to the high amount of iron along with the shape memory effect comparable to Nitinol.

Fe-SMAs do not have the same properties as Nitinol. Still, their features are like Nitinol to such an extent that they can be used as a replacement for Nitinol. The procedures of the experiment include the preparation of specimens with weights between 3mg-10mg. The samples are heat treated followed by brine quenching and the temperatures along with respective soaking times are shown in Table 2. Differential scanning calorimetry (DSC) results have been obtained and discussed, and then the conclusion is drawn. These procedures take place in the following steps

2.1 Preparation of Samples

At first, the samples of Fe-15Mn-10 Cr-8Ni-4Si (wt. %) are prepared, and its pieces are obtained by cutting with a sheet metal cutter for the procedure. The weights of the specimens range from 3mg-10mg. It is done cleanly so that no other contaminants mix up. Then these pieces are quenched after putting them under different heat conditions for a different period.

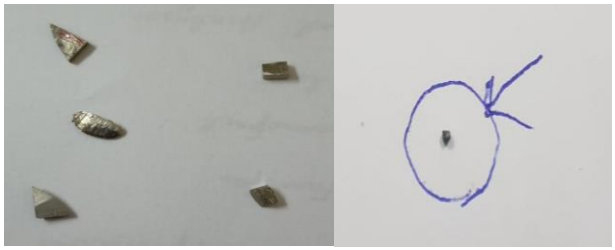

Fig. 2. Material Used in The Study Before (Left) And After Preparation (Right)

2.2. Preparation of Brine

The brine composition used for this study is 3.5% which is prepared by dissolving 21g lab-grade NaCl (salt) into 600 ml water by constant stirring. Each specimen is placed in this brine solution after the heat treatment for 10 minutes before DSC measurement. The new brine solution is used for each sample, and the brine solution is flushed away after extracting the specimen using tissue paper as filter paper.

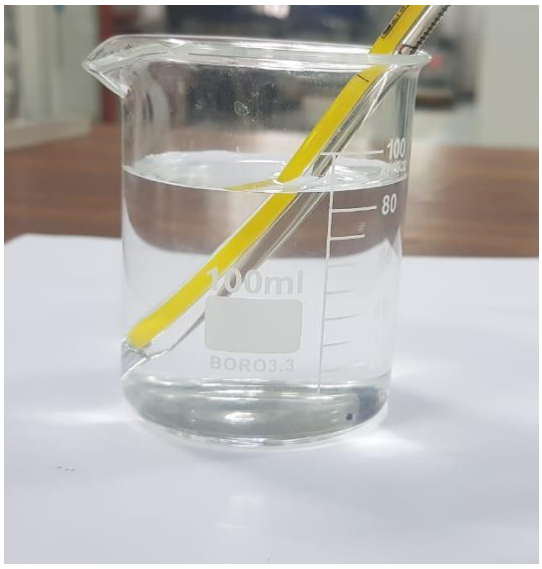

Fig. 3. Brine Solution Prepared for Quenching

2.3. Heat Treatment of the Samples

From the literature, different methods for different shape memory alloys at the low-temperature range are found. It is found that the heat processes done for this specimen at this temperature range have not been examined before. However, the heat processes have been done for this specimen which is not used for the transformation temperature decreasing purposes.

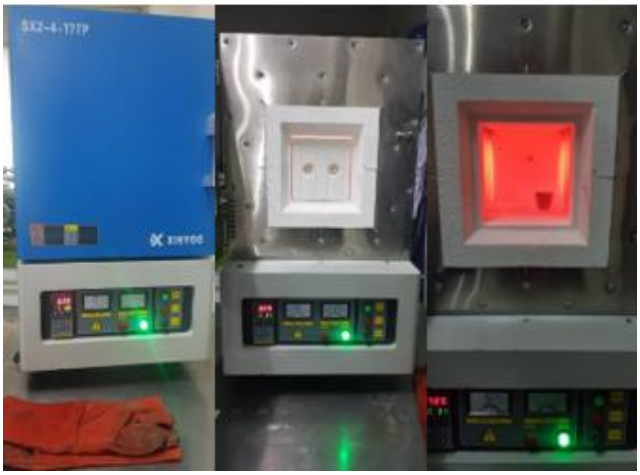

Fig. 4. Heating The Samples Using an Electric Furnace

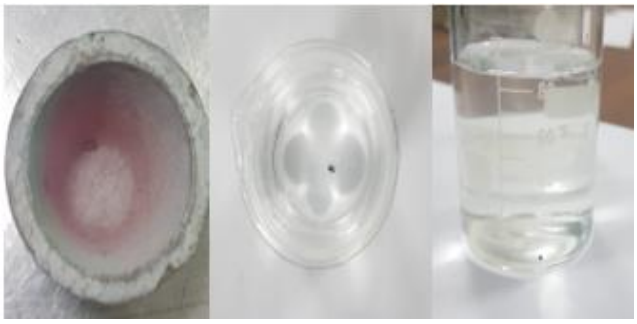

Fig. 5. DSC Sample of Fe-SMA Used in The Study Being Quenched After Heating

Table 1

Quenching scheme for Fe-15Mn-10Cr-8Ni-4Si (wt. %)

Sample #	Heating Temperature (°C)	Heating Duration (minutes)
1	600°C	30
2	600°C	60
3	600°C	90
4	700°C	25
5	700°C	50
6	700°C	75
7	800°C	10
8	800°C	30
9	800°C	50

Heat treatment, along with mechanical treatment like cold and hot working, also causes defects in the medical implants, which is not desired. Quenching is the only available facility in the methods that proved beneficial in decreasing the A_s of Fe-SMAs. So, it is decided to use quenching with a brine solution as some

results from the literature point out that quenching with a brine solution is more effective than quenching with ice water or oil [45]. After an in-depth literature review, from all the techniques mentioned above, quenching with brine solution is used in this study. In this process, the heated specimen is cooled in brine solution immediately after heating at a high temperature at a given time. The heating temperatures and respective soaking times are shown in Table 2.

3. Results and Discussions

Fig. 6 shows the microstructure of Fe-15Mn-10Cr-8Ni-4Si before heat treatment using SEM. In this image, the twin phases present in the alloy can be observed as also mentioned in Fig. 6. In this microstructure, both phases are visible and marked in the image. The phase transformation between martensite and austenite is observed using DSC.

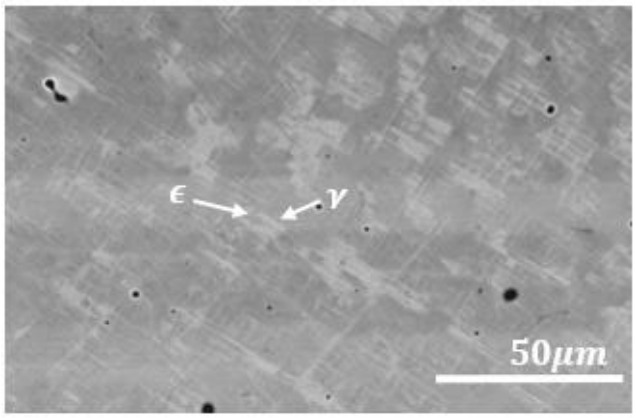

Fig. 6. SEM Result for Fe-15Mn-10Cr-8Ni-4Si Before Heat Treatment

Table 3

Results obtained after quenching of Fe-15Mn-10Cr-8Ni-4Si (wt. %)

Sample #	A_s (°C)	A_f (°C)
1	39.0°C	49.1°C
3	115.4°C	120°C

An endothermic peak in the downward direction represents the reverse transformation from martensite to austenite in the DSC curve. From the DSC endothermic peak, values of A_s and A_f are observed. The method used for the observation for A_s and A_f is observed from the literature drawing two tangent lines, one line following the DSC curve and the other line that follows the peak line, the peak starts, and this line crosses the first line. Three lines are needed to be drawn. The intersection of the first two lines gives A_s and the second line is marked on the other side of the peak when the heat flow is rising to achieve the trend of the curve and A_f is obtained. These temperature values are obtained from samples 1 and 3 as peaks are not observed from other samples.

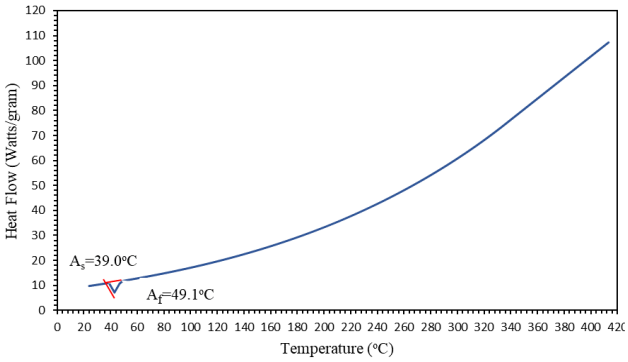

Fig. 7. DSC Curve of S1 Treated At 600 °C for 30 Minutes

In Fig. 7, the DSC curve for sample 1 is shown; the results are made after quenching the specimen at 600°C for about 30 minutes. The A_s is 39.0oC, as marked in Fig. 7, the material transforms completely after $A_f = 49.1$°C making the provided temperature directly related to the heat flow. The evidence of martensite formation is supported by the study that most Fe-SMAs have martensite start and finish temperatures above room temperature [43].

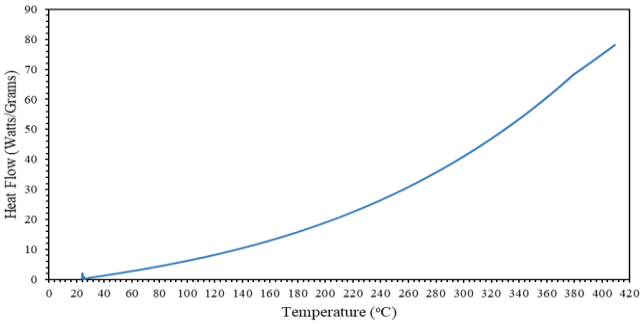

Fig. 8. DSC Curve of S2 and S4 Treated at 600 °C and 700 °C for 60 Minutes And 35 Minutes Respectively

In Fig. 8, the DSC curves for samples 2 and 4 are shown as both are very similar. These samples are heated at 600°C and 700°C for 60 and 25 minutes, respectively. There is a slight irregularity in the curve at a high temperature of about 380-400°C. A_s and A_f have not been observed in this case, the curve is almost as smooth as in the previous case.

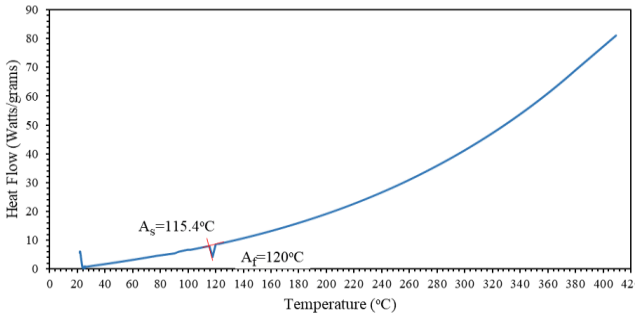

Fig. 9. DSC Curve of S3 at 600 °C for 90 Minutes

In Fig. 9, the DSC curve for sample 3 is shown. The sample is heated at 600°C for 90 minutes. From the start to about 115°C, Fig. shows a direct relationship between temperature and heat flow. After

that, at 115.4℃, the material transforms, and the austenite temperature starts at this point. The austenite state is sustained to about 120℃. This is the A_f of the sample undergoing quenching at 600℃ for 60 minutes. The smoothness of the curve is similar to sample 1.

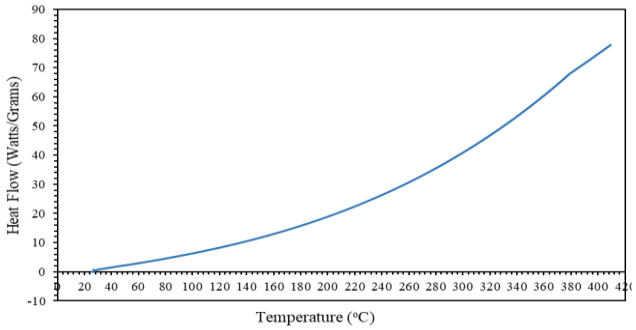

Fig. 10. DSC Curve of S5 Treated at 700 ºC for 50 Minutes

In Fig. 10, the DSC curve for sample 5, where the sample is quenched for 700℃, but for 50 minutes. A_s and A_f are not observed in this case as well. By looking at the curve, it is observed that the irregularity in this curve starts a little earlier than the irregularity occurring in the previous case. The irregularity occurs at 365-375℃ in this Fig. However, the steepness is almost the same.

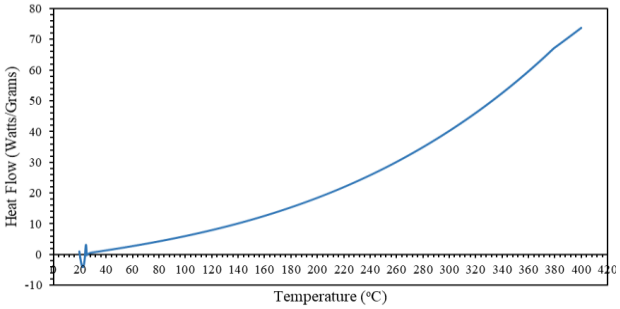

Fig. 11. DSC Curve of S6 and S7 at 700 ºC and 800 ºC for 75 Minutes and 10 Minutes Respectively

In Fig. 11, the DSC curves for samples 6 and 7 are shown as they were similar. The quenching temperature for this case is also 700℃ and 800ºC. The A_s and A_f are not observed in this case. The only difference perceived for this case compared to the above ones is the steepness of the curve is almost the same, but the irregularity interval is a little greater than in the previous case; the irregularity starts at about 376℃ and ends at about 390℃. This has little effect on the smoothness of the curve.

In Fig. 12, the DSC curves for samples 8 and 9 are shown as they were similar. These samples are heated at 800℃ for 30 and 50 minutes. The A_s and A_f are not observed in this case.

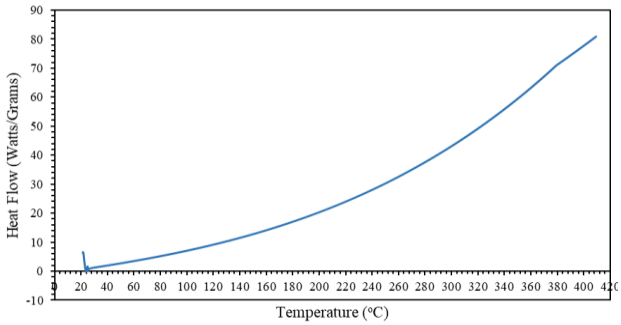

Fig. 12. DSC Curve of S8 and S9 Treated at 800 ºC for 30 Minutes And 50 Minutes Respectively

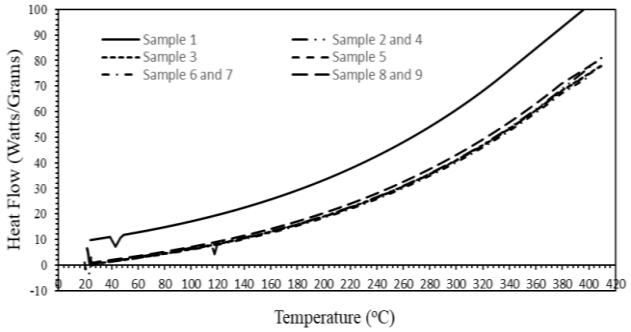

Fig. 13. DSC Curves of Fe-SMA Samples After Quenching With 3.5% Brine Solution

Fig. 13 represents the comparison of all the curves concerning their quenching temperatures and the amount of time induced. After observing the Fig, it can be observed that the curves of the figures with low quenching temperatures stand higher than the ones with comparatively high quenching temperatures. The amount of time the sample has been put after the quenching temperature has a mild effect on the curve. Thus, it can be interpreted that the more time the sample has been placed after the quenching temperature, the lower the curve would be. The cases where the quenching temperature is 800℃ show a negligible difference in Fig. 13.

Although, Fig. 13 also shows that the higher the quenching temperature is, the more chances of irregularities at high temperatures occur. It is also evident in this Fig. that the curve of the case with quenching temperature at 600℃ for 30 minutes stands highest above all other curves. Its A_s is the lowest, as well as the austenite finish temperature. Since the required temperature for the A_s should be around the normal human body temperature, this Fig. is preferably the most suited case. The one possible reason for the absence of the DSC peaks is that the crystallisation growth is too slow or too fast to be observed by DSC.

The alloy used in this study is of the composition Fe-15Mn-10Cr-8Ni-4Si (wt. %). Using the same composition gives us the advantage of analysing the effect of thermal treatment effectively while considering the effect of the composition. One of the

major components includes manganese which controls the gamma phase, and its concentration affects the phase transformation. If it is in a higher amount in an alloy, it causes the alloy to be less corrosion-resistant and less resistant to high-temperature oxidation. Silicon with less amount in an alloy tends to increase the resistance to high-temperature oxidation. But, it causes brittleness limiting the cold working. Chromium also improves corrosion resistance and oxidation resistance but excess amount of chromium has disadvantages such as if it exceeds 11%, it tends to decrease the stacking fault energy and toughness and workability if its amount increases beyond 20% [11]. Nickel inhibits ferrite formation without stabilising the austenite phase, and an excess amount of Ni depresses the martensitic temperature.

4. Conclusion

Nitinol has various applications in the biomedical field and other engineering applications. Due to the high cost of Nitinol, the researchers are working on getting a cheaper solution in other shape memory alloys with similar or at least comparable properties and biocompatibility with corrosion resistance. Fe-SMAs are capable of this purpose as they are cheap, ductile, biodegradable, biocompatible, and corrosion-resistant as well as possessing high mechanical strength and shape memory properties comparable to that of Nitinol, however, high transformation temperatures of Fe-SMAs are the main limiting factor for their feasibility in human body applications. There are not many techniques developed so far to reduce A_s, which is one of the primary concerns in human body implant applications. Quenching technique amongst other heat treatment processes is observed advantageous to reduce A_s considerably for Cu-SMAs. In this study, 3.5% brine solution is used for quenching the heat-treated Fe-15Mn-10 Cr-8Ni-4Si (wt. %) samples to reduce their A_s. From the DSC results of this paper, the maximum reduction in A_s resulted from 93°C to 39.02°C for the sample which is heat-treated at 600°C for 30 minutes in an electric furnace followed by brine quenching. It has been concluded that the reduced A_s is 39.02°C which is close to the human body temperature which can make this cheaper biocompatible alloy successful for human body applications.

5. References

[1] J. D. W. Madden, “Dielectric elastomers as high-performance electroactive polymers”, Dielectr. Elastomers as Electromechanical Transducers, 2008.

[2] H. Khodaverdi, M. Mohri, E. Ghafoori, A. S. Ghorabaei, and M. Nili-Ahmadabadi, “Enhanced pseudoelasticity of an Fe-Mn-Si-based shape memory alloy by applying microstructural engineering through recrystallization and precipitation”, J. Mater. Res. Technol., vol. 21, pp. 2999–3013, 2022, doi: 10.1016/j.jmrt.2022.10.092.

[3] D. Stöckel, “The shape memory effect - Phenomenon, alloys, applications”, Proc. Shape Mem. Alloy. Power Syst., pp. 25–61, Jan. 2000, doi: 10.1007/978-3-662-09875-2_3.

[4] H. Rojob, “Innovative near-surface mounted iron-based shape memory alloy for strengthening structures innovative near-surface mounted iron-based shape memory alloy for strengthening structures by a thesis © Hothifa N Rojob 2017”, no. January, 2019, doi: 10.11575/PRISM/26542.

[5] L. G. Bujoreanu, S. Stanciu, R. I. Comaneci, M. Meyer, V. Dia, and C. Lohan, “Factors influencing the reversion of stress-induced martensite to austenite in a Fe-Mn-Si-Cr-Ni shape memory alloy”, J. Mater. Eng. Perform., vol. 18, no. 5–6, pp. 500–505, 2009, doi: 10.1007/s11665-009-9499-2.

[6] Q. Sun, B. Cao, T. Iwamoto, and T. Suo, “Effect of impact deformation on shape recovery behavior in Fe-Mn-Si shape memory alloy under shape memory training process with cyclic thermo-mechanical loading”, Sci. China Technol. Sci., vol. 64, pp. 1389–1400, 2021.

[7] M. Vollmer et al., “On the effect of gamma phase formation on the pseudoelastic performance of polycrystalline Fe-Mn-Al-Ni shape memory alloys”, Scr. Mater., vol. 108, pp. 23–26, 2015, doi: 10.1016/j.scriptamat.2015.06.013.

[8] B. C. Maji and M. Krishnan, “Effect of copper addition on the microstructure and shape recovery of Fe-Mn-Si-Cr-Ni shape memory alloys”, Mater. Sci. Eng. A, vol. 570, pp. 13–26, 2013, doi: 10.1016/j.msea.2013.01.061.

[9] Y. Sakuma, O. Matsumura, and H. Takechi, “Mechanical properties and retained austenite in intercritically heat-treated bainite-transformed steel and their variation with Si and Mn additions”, Metall. Trans. A, vol. 22, no. 2, pp. 489–498, 1991, doi: 10.1007/BF02656816.

[10] N. Van Caenegem, L. Duprez, K. Verbeken, B. C. De Cooman, Y. Houbaert, and D. Segers, “Effect of carbon on the shape memory mechanism in FeMnSiCrNi SMAs”, ISIJ Int., vol. 47, no. 5, pp. 723–732, 2007, doi: 10.2355/isijinternational.47.723.

[11] Q. Gu, J. Van Humbeeck, and L. Delaey, “Review on the martensitic transformation and shape memory effect in Fe-Mn-Si alloys”, J. Phys. IV JP, vol. 4, no. 3, pp. 135–144, 1994, doi: 10.1051/jp4:1994319.

[12] Q. Sun, B. Cao, and T. Iwamoto, “Whole martensitic transformation process in Fe–Mn–Si–Cr shape memory alloy by improved characterization of volume resistivity”, J. Mater. Res. Technol., vol. 25, pp. 2061–2074, 2023.

[13] X. X. Wang and C. Y. Zhang, “Pseudoelastic behavior in an Fe-Mn-Si-Ni-Co shape memory alloy”, J. Mater. Sci. Lett., vol. 17, no. 21, pp. 1795–1796, 1998, doi: 10.1023/A:1006605519929.

[14] L. J. Rong, Y. Y. Li, and C. X. Shi, “Improvement of shape memory effect in an Fe-Mn-Si-Cr-Ni alloy”, Scr. Mater., vol. 34, no. 6, pp. 993–998, 1996, doi: 10.1016/1359-6462(95)00605-2.

[15] A. Akhondzadeh, K. Zangeneh-Madar, and S. M. Abbasi, “Influence of annealing temperature on the shape memory effect of Fe-14Mn-5Si-9Cr-5Ni alloy after training treatment”, Mater. Sci. Eng. A, vol. 489, no. 1–2, pp. 267–272, 2008, doi: 10.1016/j.msea.2007.12.014.

[16] O. Eyercioglu, E. Kanca, M. Pala, and E. Ozbay, “Prediction of martensite and austenite start temperatures of the Fe-based shape memory alloys by artificial neural networks”, J. Mater. Process. Technol., vol. 200, no. 1–3, pp. 146–152, 2008, doi: 10.1016/j.jmatprotec.2007.09.085.

[17] K. Tanaka and T. Watanabe, “Transformation conditions in an Fe-based shape memory alloy: an experimental study”, Arch. Mech., vol. 51, no. Transformation conditions in an Fe-based shape memory alloy: an experimental study, pp. 805–832, 1999, [Online]. Available: http://rcin.org.pl.

[18] W. J. Lee, B. Weber, G. Feltrin, C. Czaderski, M. Motavalli, and C. Leinenbach, “Phase transformation behavior under uniaxial deformation of an Fe-Mn-Si-Cr-Ni-VC shape memory alloy”, Mater. Sci. Eng. A, vol. 581, pp. 1–7, 2013, doi: 10.1016/j.msea.2013.06.002.

[19] B. Cao and T. Iwamoto, “A new method to measure volume resistivity during tension for strain rate sensitivity in deformation and transformation behavior of Fe-28Mn-6Si-5Cr shape memory alloy”, Int. J. Mech. Sci., vol. 146, pp. 445–454, 2018.

[20] B. Cao and T. Iwamoto, “An experimental investigation on rate dependency of thermomechanical and stress-induced martensitic transformation behavior in Fe-28Mn-6Si-5Cr shape memory alloy under compression”, Int. J. Impact Eng., vol. 132, p. 103284, 2019.

[21] W. J. Lee, B. Weber, G. Feltrin, C. Czaderski, M. Motavalli, and C. Leinenbach, “Stress recovery behaviour of an Fe–Mn–Si–Cr–Ni–VC shape memory alloy used for prestressing”, Smart Mater. Struct., vol. 22, no. 12, p. 125037, 2013, doi: 10.1088/0964-1726/22/12/125037.

[22] J. Pons, E. Cesari, C. Seguí, F. Masdeu, and R. Santamarta, “Ferromagnetic shape memory alloys: Alternatives to Ni-Mn-Ga”, Mater. Sci. Eng. A, vol. 481–482, no. 1-2 C, pp. 57–65, 2008, doi: 10.1016/j.msea.2007.02.152.

[23] F. Nishimura, N. Watanabe, and K. Tanaka, “Back stress and shape recoverability during reverse transformation in an Fe-based shape memory alloy”, Mater. Sci. Eng. A, vol. 247, no. 1–2, pp. 275–284, 1998, doi: 10.1016/s0921-5093(97)00841-1.

[24] K. W. K. K. Yeung, K. M. C. C. Cheung, W. W. Lu, and C. Y. Chung, “Optimization of thermal treatment parameters to alter austenitic phase transition temperature of NiTi alloy for medical implant”, Mater. Sci. Eng. A, vol. 383, no. 2, pp. 213–218, 2004, doi: 10.1016/j.msea.2004.05.063.

[25] A. Gruzdkov, S. Krivosheev, Y. Petrov, A. Razov, and A. Utkin, “Martensitic inelasticity of TiNi-shape memory alloy under pulsed loading”, Mater. Sci. Eng. A, vol. 481–482, no. 1-2 C, pp. 105–108, 2008, doi: 10.1016/j.msea.2007.03.113.

[26] R. Santhanam, Y. Krishna, and M. Sivakumar, “Influence of specimen location and residual stress on transformation temperatures of SMA spring”, Mater. Today Proc., vol. 5, no. 9, pp. 18011–18015, 2018, doi: 10.1016/j.matpr.2018.06.134.

[27] J. Olbricht, A. Yawny, A. M. Condó, F. C. Lovey, and G. Eggeler, “The influence of temperature on the evolution of functional properties during pseudoelastic cycling of ultra fine grained NiTi”, Mater. Sci. Eng. A, vol. 481–482, no. 1-2 C, pp. 142–145, 2008, doi: 10.1016/j.msea.2007.01.182.

[28] K. Wada and Y. Liu, “Thermomechanical training and the shape recovery characteristics of NiTi alloys”, Mater. Sci. Eng. A, vol. 481–482, no. 1-2 C, pp. 166–169, 2008, doi: 10.1016/j.msea.2007.02.143.

[29] C. Grabe and O. T. Bruhns, “Tension/torsion tests of pseudoelastic, polycrystalline NiTi shape memory alloys under temperature control”, Mater. Sci. Eng. A, vol. 481–482, no. 1-2 C, pp. 109–113, 2008, doi: 10.1016/j.msea.2007.03.117.

[30] C. Lexcellent, P. Blanc, and N. Creton, “Two ways for predicting the hysteresis minimisation for shape memory alloys”, Mater. Sci. Eng. A, vol. 481–482, no. 1-2 C, pp. 334–338, 2008, doi: 10.1016/j.msea.2007.03.120.

[31] Y. S. Kim, E. Choi, and W. J. Kim, “Characterization of the microstructures and the shape memory properties of the Fe-Mn-Si-Cr-Ni-C shape memory alloy after severe plastic deformation by differential speed rolling and subsequent annealing”, Mater. Charact., vol. 136, no. December 2017, pp. 12–19, 2018, doi: 10.1016/j.matchar.2017.11.055.

[32] L. Wang, L. J. Rong, D. S. Yan, Z. M. Jiang, and Y. Y. Li, “DSC study of the reverse martensitic transformation behavior in a shape memory alloy pipe-joint”, Intermetallics, vol. 13, no. 3–4, pp. 403–407, 2005, doi: 10.1016/j.intermet.2004.07.025.

[33] K. Prusik, B. Kostrubiec, T. Goryczka, G. Dercz, P. Ochin, and H. Morawiec, “Effect of composition and heat treatment on the martensitic transformations in Co-Ni-Ga alloys”, Mater. Sci. Eng. A, vol. 481–482, no. 1-2 C, pp. 330–333, 2008, doi: 10.1016/j.msea.2007.01.187.

[34] H. Jiang et al., “Martensitic transformation and shape memory effect at high temperatures in off-stoichiometric Co2VSi Heusler alloys”, Mater. Sci. Eng. A, vol. 676, pp. 191–196, 2016, doi: 10.1016/j.msea.2016.08.083.

[35] B. Cao, Q. Sun, and T. Iwamoto, “Effect of deformation rate on the axial joint strength made of Fe-SMA”, J. Constr. Steel Res., vol. 191, p. 107193, 2022.

[36] B. Cao, Q. Sun, and T. Iwamoto, “Bending fracture strength of the pipe joint using iron-based shape memory alloy (Fe-SMA) subjected to different expansion methods at various deformation rates”, Eng. Struct., vol. 267, p. 114669, 2022.

[37] B. Cao and T. Iwamoto, “A strength prediction of joints by Fe-Mn-Si-Cr shape memory alloy through strain monitoring during pre-processes including diameter expansion and tightening by heating”, Eng. Fract. Mech., vol. 284, p. 109234, 2023.

[38] B. Liu, Y. F. Zheng, and L. Ruan, “In vitro investigation of Fe30Mn6Si shape memory alloy as potential biodegradable metallic material”, Mater. Lett., vol. 65, no. 3, pp. 540–543, 2011, doi: 10.1016/j.matlet.2010.10.068.

[39] A. Francis, Y. Yang, S. Virtanen, and A. R. Boccaccini, “Iron and iron-based alloys for temporary cardiovascular applications”, J. Mater. Sci. Mater. Med., vol. 26, no. 3, pp. 1–16, 2015, doi: 10.1007/s10856-015-5473-8.

[40] S. Gautam, D. Bhatnagar, D. Bansal, H. Batra, and N. Goyal, “Recent advancements in nanomaterials for biomedical implants”, Biomed. Eng. Adv., vol. 3, no. March, p. 100029, 2022, doi: 10.1016/j.bea.2022.100029.

[41] B. C. Maji, C. M. Das, M. Krishnan, and R. K. Ray, “The corrosion behaviour of Fe-15Mn-7Si-9Cr-5Ni shape memory alloy”, Corros. Sci., vol. 48, no. 4, pp. 937–949, 2006, doi: 10.1016/j.corsci.2005.02.024.

[42] R. A. Rahman, D. Juhre, and T. Halle, “Review of Applications of Ferrous Based Shape Memory Smart Materials in Engineering and in Biomedical Sciences”, Pakistan J. enginnering Appl. Sci., vol. 24, no. 5, pp. 32–49, 2019.

[43] R. Atta, D. Halle, and T. Mehmood, “Types , DSC thermal characterization of Fe-Mn-Si based shape memory smart materials and their feasibility for human body in terms of austenitic start temperatures”, J. Eng. Technol., vol. 8, no. 1, pp. 185–206, 2019.

[44] W. Jiang, W. Zhao, T. Zhou, L. Wang, and T. Qiu, “A review on manufacturing and post-processing technology of vascular stents”, Micromachines, vol. 13, no. 1, 2022, doi: 10.3390/mi13010140.

[45] S. N. Saud, E. Hamzah, T. Abubakar, and S. Farahany, “Structure-property relationship of Cu-Al-Ni-Fe shape memory alloys in different quenching media”, J. Mater. Eng. Perform., vol. 23, no. 1, pp. 255–261, 2014, doi: 10.1007/s11665-013-0759-9.

